J. Physiol. (1984), **348**, *pp.* 187–207
With 11 *text-figures*
Printed in Great Britain

CALCIUM CURRENT ACTIVATION KINETICS IN NEURONES OF THE SNAIL *LYMNAEA STAGNALIS*

BY LOU BYERLY, P. BRYANT CHASE AND JOSEPH R. STIMERS*

From the Department of Biological Sciences, University of Southern California, Los Angeles, CA 90089, U.S.A.

(*Received 11 May 1983*)

SUMMARY

1. Both the activation kinetics and the magnitude of the Ca current in *Lymnaea* are strongly dependent on temperature. The Q_{10} for the reciprocal of the activation time constant is $4{\cdot}9 \pm 0{\cdot}2$ and the Q_{10} for the maximum current is $2{\cdot}3 \pm 0{\cdot}1$. By lowering the temperature to 7–10 °C, we have been able to resolve the Ca tail currents.

2. The block of Ca current by Cd^{2+} is voltage dependent, being more effective at more positive potentials.

3. As determined from the magnitude of the tail currents, the Ca permeability is not maximally activated until the membrane potential is greater than +70 mV. The Ca permeability is half activated in the range 30–35 mV.

4. The open-channel current–voltage relation for the Ca current is in rough agreement with the prediction of the constant-field equation. There is no indication of current saturation at negative potentials for potentials down to −60 mV.

5. The Ca tail current decays with at least two time constants, one 200–400 μs and the other 2–4 ms. Although these time constants are not strongly voltage dependent, the ratio of the amplitude of the fast component of the tail current to that of the slow component is much larger at −60 mV than at 0 mV. The time course of the Ba tail current is very similar to that of the Ca tail current.

6. The time course of the activation of the Ca current follows m^2 kinetics and does not show evidence for a Cole–Moore-type shift for holding potentials between −50 and −110 mV. During a second positive pulse applied 1 ms after the first, the Ca current activates more rapidly, without the delay characteristic of the Ca current of a single positive pulse.

7. The activation of the Ca current can be represented by a linear sequential model. The simplest model that describes both the turn-on and the turn-off of the Ca current must have at least three closed states, followed by a single open state.

INTRODUCTION

The study of the kinetics of Ca current activation has been considerably limited by the slow nature of the voltage clamps obtained when micro-electrode techniques

* Present Address: Department of Physiology, U.C.L.A. Medical School, Los Angeles, CA 90024, U.S.A.

are applied to cells of complicated geometry. However, in the last decade a number of new techniques have been developed which provide considerably faster control of the potential of certain membranes that pass Ca currents. All of these techniques involve sealing the membrane of an isolated spherical cell to a suction electrode with an opening which is an appreciable fraction ($\frac{1}{20}$–$\frac{1}{3}$) of the cell diameter and then breaking the patch of membrane under the electrode (Krishtal & Pidoplichko, 1975; Lee, Akaike & Brown, 1978; Takahashi & Yoshii, 1978; Hamill, Marty, Neher, Sakmann & Sigworth, 1981). Following a positive step in membrane potential, the Ca current activates with a sigmoidal time course that is well described by m^2 kinetics. This has been shown in snail neurones (Kostyuk, Krishtal & Shakhovalov, 1977; Kostyuk, Krishtal & Pidoplichko, 1981; Byerly & Hagiwara, 1982) and clonal pituitary cells (Hagiwara & Ohmori, 1982). The Ca current in chromaffin cells also activates with a sigmoidal time course, but Fenwick, Marty & Neher (1982) have fitted a three-exponential expression to the data. Byerly & Hagiwara (1981, 1982) found that, when the membrane is repolarized, the Ca current turns off with a time course that is much faster than expected from the activation time course; however, in their studies of snail neurone Ca currents at room temperature the tail currents were too fast to be accurately measured. Subsequently, the Ca tail currents in snail neurones (Tsuda, Wilson & Brown, 1982) and chromaffin cells (Fenwick *et al.* 1982) were found to have two components, one with a time constant similar to that of Ca current activation and a second one that was much smaller. These indications of the presence of a faster process in Ca current activation have been supported by results from studies of single-channel Ca recording. In snail neurones (Lux & Nagy, 1981), cardiac cells (Reuter, Stevens, Tsien & Yellen, 1982), chromaffin cells (Fenwick *et al.* 1982), and pituitary cells (Hagiwara & Ohmori, 1983), the single-channel Ca current has been found to flicker on and off with a time course that is considerably faster than that of the activation of the macroscopic current.

In this paper, we report studies of macroscopic Ca currents in *Lymnaea* neurones at 7–10 °C; at these lower temperatures, the Ca current kinetics are slowed sufficiently to provide clear resolution of the Ca tail current. Accurate measurement of the Ca tail currents allows us to study in considerably greater detail the activation gating mechanism of Ca channels.

METHODS

All experiments were done using the internal-perfusion voltage-clamp technique on isolated nerve cell bodies of *Lymnaea stagnalis*. The methods used are those of Byerly & Hagiwara (1982). Due to the reduced size of the Ca currents at the low temperatures used in these studies, only the largest nerve cell bodies of *Lymnaea* were used, 100–120 μm in diameter. The largest Ca currents tend to be found in the largest cells.

Voltage clamp

Since it was essential to be able to change the membrane potential rapidly in these studies, all experiments were done with the hybrid clamp configuration, i.e. recording potential with a micro-electrode inserted into the cell while injecting current through the suction electrode. To increase the speed of the clamp, we reduced the resistances of the suction electrode and micro-electrode as much as possible. The diameter of the opening of the suction electrode was about one-third that of the cell (32–40 μm), giving a resistance of 200–300 kΩ when filled with the internal solution. The micro-electrodes were filled with 3 M-KCl and had a resistance of about 5 MΩ. The

most critical test of the speed of the clamp was to measure the time at which the Ca tail current reached a peak, when the membrane potential was stepped back from positive potentials to the holding potential. In an ideal voltage clamp, there would be no delay between the beginning of the step down in potential and the peak of the Ca tail current. Occasionally we obtained delays less than 100 μs, but more typically the delay was 150–200 μs.

Solutions

The external solution contained 4 mM-Ca^{2+}, 4 mM-Mg^{2+}, 65 mM-Tris, 10 mM-4-aminopyridine, and 74 mM-Cl^{-}; the pH was adjusted to 7·4 with HCl. The internal solution contained 74 mM-Cs^{+}, 62 mM-aspartate, 5 mM-HEPES, and 5 mM-EGTA, the pH was adjusted to 7·3 with CsOH. In some experiments, the external solution was modified in the following ways: to study Ba currents, 4 mM-Ca^{2+} was replaced by 4 mM-Ba^{2+}; to block Ca current, 0·1 mM-Cd^{2+} was added, or 3 mM-Co^{2+} replaced 3 mM-Mg^{2+}; Ca tail current was eliminated by replacing all Ca^{2+} and Mg^{2+} by 8 mM-Co^{2+}; to vary Ca current size, 4 mM-Mg^{2+} was replaced by 4 mM-Ca^{2+}, or 3 mM-Ca^{2+} by 3 mM-Mg^{2+}.

Temperature control

The temperature of the external solution was lowered by passing it through an ice bath before it entered the recording chamber. The temperature was monitored by a thermistor in the bath. The temperature varied by less than 1 °C during an experiment. To determine the temperature sensitivity of the Ca current, temperature was varied by changing the flow rate of the external solution.

Data collection

Current and voltage records were digitized with 12-bit resolution at intervals of 10–100 μs. To prevent saturation of the A–D converter by the capacitive transient, a two-exponential signal generated from the voltage command signal was applied to the input of the current–voltage converter through a small capacitor. The amplitudes and time constants of both exponentials were adjusted so as to minimize the recording of the capacitive transient. In all experiments, pairs of voltage command signals of equal magnitude but opposite polarity were applied consecutively ($\pm$P procedure). The two current records obtained from each pair of signals were added, thus producing a current record that was relatively free of capacitive and linear leakage currents. These summed currents were stored on floppy disk for later analysis. All current records shown in this paper are such summed currents, plotted by the computer on an X–Y plotter.

Data fitting

All fits were done by transforming the data into a linear form and then using a least-squares fit to a straight line, weighting the data according to the transformation that had been applied to linearize them. In fitting tail currents, an initial value for the constant term was obtained from the current at 8 ms (after the step in potential). The data between 2 and 8 ms were fitted by a single exponential plus the constant term. This fit was used to calculate a second and final value for the constant term, which was then used on the same data to obtain the final fit for the slow component of the tail current. Subtracting the projection of these terms to earlier times, the remainder for the data between 200 μs and 2 ms was fitted to a single exponential to determine the fast time constant.

In fitting the activation of Ca currents, we take zero time to be about 100 μs after the pulse beginning, which is the time required for the membrane potential to reach the command level. The fit is made to the data from zero time to the time at which the current reaches the steady-state value. We interpret the small outward current (I_{so}) which is seen before the activation of the Ca current at more positive potentials to be the non-linear leakage current that is still seen after the Ca current is completely gone; this leakage current is time-independent except for a rapid turn-on. We assume gating currents are negligibly small, although they are undoubtedly present. If the current obtained after applying 0·1 mM-Cd^{2+} is subtracted from the Ca current recorded before applying Cd^{2+}, a difference current is obtained which shows no jump (no I_{so}) at the beginning of the voltage pulse (see Fig. 2). The time course of this difference current is very similar to that of the unsubtracted record measured from the level of I_{so}. Since the difference current is noisier and requires measuring the currents in Cd^{2+}, we have chosen to analyse the time course of the unsubtracted Ca current, taking zero current to be the level of I_{so}.

RESULTS

Temperature dependence

Both the size and the time course of the Ca current in *Lymnaea* cell bodies are very sensitive to temperature. In order to quantify this temperature dependence, cells were studied under hybrid voltage clamp (see Methods), but using a small-opening (10–15 μm) suction electrode. This provided a control of the membrane potential that was sufficiently fast to resolve the activation of the Ca current, but greatly reduced the rate of internal perfusion. After the K^+ inside the cell had been replaced by Cs^+,

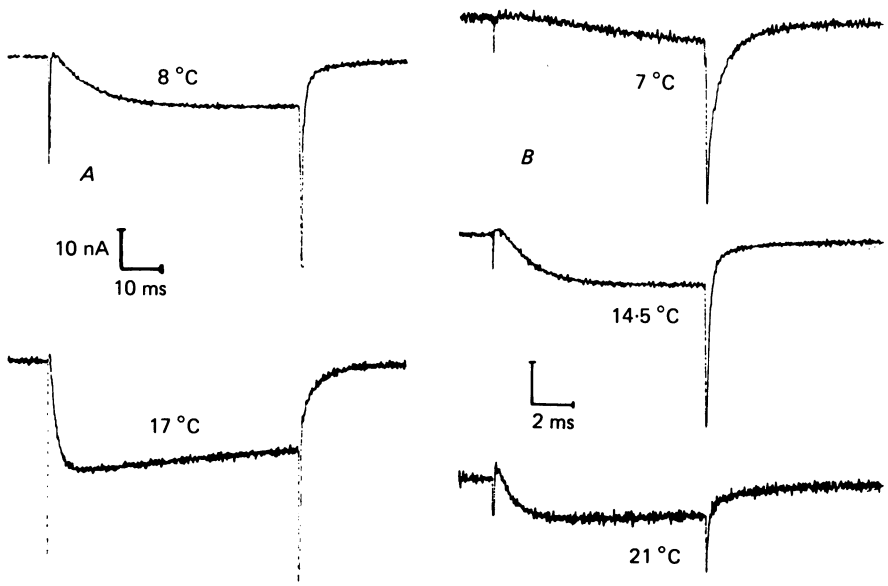

Fig. 1. Temperature dependence of Ca current. All current records taken during a pulse to +20 mV from the holding potential of −50 mV. *A*, two current records taken from the same cell at 17 and 8 °C. Suction electrode diameter was 12 μm. Pulse duration 60 ms. Calibration: 10 nA by 10 ms. *B*, three current records taken from a single cell during warming. From top to bottom: 7, 14·5 and 21 °C. Current low-pass filter set at 10 kHz. Suction electrode diameter was 40 μm, so Ca current showed considerable wash-out in last trace (21 °C). Pulse duration was 10 ms. Calibration: 10, 20 and 10 nA (top to bottom) by 2 ms.

which required 10–15 min with the small suction electrode, the Ca current showed very little wash-out (Byerly & Hagiwara, 1982) over the next hour, allowing time for four to six temperature changes. Only data from those cells in which the Ca current returned to its initial size on returning to the initial temperature were used to calculate the temperature dependence. The temperature was varied between 7 and 21 °C.

As can be seen in Fig. 1*A*, the size of the Ca current is smaller at a lower temperature. Both of these current records were obtained at +20 mV, which is the voltage that gives the maximum Ca current at each temperature. This 9° drop in temperature reduced the Ca current by more than a factor of 2. The Q_{10} for the maximum Ca current measured in five cells was 2·3 ± 0·1 (mean ± S.D.). The 9° drop

in temperature also increased the time required for the Ca current to reach half of its peak value ($t_{\frac{1}{2}}$) from 1·7 to 8·9 ms. The Q_{10} for the reciprocal of $t_{\frac{1}{2}}$ measured in three cells was $4{\cdot}9 \pm 0{\cdot}2$ (mean $\pm$ S.D.).

It was not possible to quantify the temperature dependence of the time course of the Ca tail current, because it is too fast at temperatures above 15 °C to be clearly resolved by our voltage clamp. However, the current records in Fig. 1*B*, which are taken from one cell at three different temperatures, clearly show that the tail current is considerably slower at lower temperatures. A suction electrode with the normal large opening (40 μm) was used in this case to give the fastest control of membrane potential possible. Since the membrane potential change occurs with the same time course in all three records of Fig. 1*B*, the relative rate of decay of the tail current can be estimated by the ratio of the size of the peak tail current to the inward current just before the tail. The peak tail current at 7 °C (top record) is 8 times the size of the inward current at the end of the +20 mV pulse, while the peak tail current at 21 °C (bottom record) is no larger than twice the inward current at the end of the pulse. This indicates that the rate of closure of Ca channels at the end of the positive voltage pulse is also temperature dependent in this range.

All the experiments described in the following sections of this paper were done at temperatures between 7 and 10 °C. Although this causes the size of the Ca current to be reduced to only 30 % of its size at room temperature, it slows down the turn-on of the Ca current by a factor of 7–10 and slows the turn-off sufficiently to allow a clear resolution of the Ca tail current. An additional advantage to studying the Ca current at low temperature is that the current is much more stable with time at these temperatures. There is a rapid wash-out of Ca current with internal perfusion at room temperature (Byerly & Hagiwara, 1982); however, at 7–10 °C, the rate of Ca current wash-out is greatly reduced. Thus it was possible to study the Ca current for a half-hour period with almost no change in the magnitude of the Ca current.

Identification of Ca tail current

The prominent inward tail current recorded during the first few milliseconds following the end of the positive pulse is the Ca tail current. In other words, this early tail current passes through the same voltage-dependent channels that carry the Ca current seen during the positive pulse. It is important to make this identification because, even in the absence of K^+ and Na^+ on both sides of the membrane, there are still time-dependent, voltage-dependent currents in snail nerve cell membranes that are not carried by Ca^{2+} (Kostyuk *et al.* 1977). It has been shown for *Lymnaea* neurones at 25 °C in solutions identical to those used here that the tail currents measured at times greater than 1 ms following the end of the positive pulse are primarily carried by ions other than Ca^{2+} (Byerly & Hagiwara, 1982). However, at the low temperatures (7–10 °C) at which the remaining studies of this paper were done, the decay of the very large Ca tail current was slowed so that it dominates the first 3–4 ms following the end of the positive pulse. We have reached this conclusion based on a number of results that are reported below.

The magnitude of the early tail current (0–3 ms) increases with increasing duration of the positive pulse in a way that parallels the time course of the activation of the Ca current recorded during the positive pulse. Fig. 2 shows five overlapping current

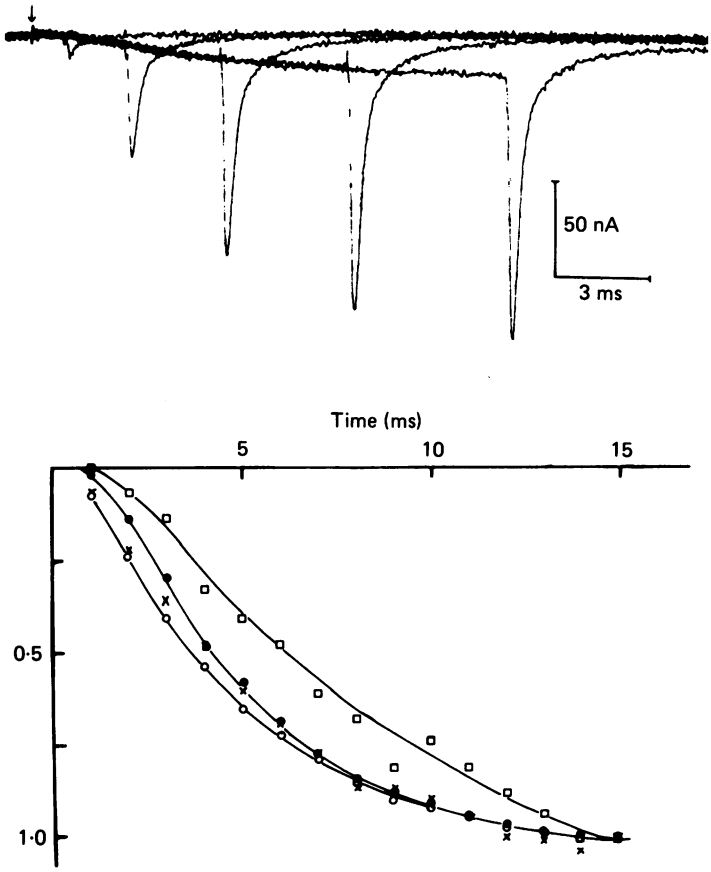

Fig. 2. Development of tail current with pulse duration. Five current records taken during pulses to +40 mV. Pulse durations were 1, 3, 6, 10 and 15 ms. Arrow indicates the beginning of each pulse. Holding potential was −50 mV. Low-pass filter set at 10 kHz. These current records are the difference of records obtained before and after 0·1 mM-Cd; this subtraction is done to clarify the time course of the Ca current during the pulse. Below, data from these and additional records are plotted on a normalized scale. The current measured at the end of a pulse to +40 mV (●) is taken from the Cd-subtracted records; the tail current at the peak (○), at 1·5 ms (×), and at 6 ms (□) are all measured from the records before the Cd subtraction.

records that illustrate this point. The Ca current measured just before the end of the pulse (●) has a very similar time course to that of the tail current, measured at the peak (○) or at 1·5 ms (×) following the end of the voltage pulse. However, the tail current measured at 6 ms (□) has a somewhat different time course, probably indicating that tail currents flowing through channels other than the Ca channel are no longer negligible at this late time.

Alterations in the external solution affect the early tail current in the same way that they affect the Ca current during the positive pulse. The magnitude of the early tail current varies directly with the external Ca^{2+} concentration $[Ca^{2+}]_o$, although not linearly. An increase of $[Ca^{2+}]_o$ from 1 to 8 mM causes the early tail current to become 3–4 times larger. The Ca channel blockers Cd^{2+} and Co^{2+} are effective in blocking the

early tail current. Co^{2+} blocks the peak tail current recorded at the end of a positive pulse to the same extent as it blocks the Ca current recorded during the pulse. If all external Ca^{2+} and Mg^{2+} are replaced by Co^{2+}, both the inward current during the pulse and the tail current are eliminated (Fig. 3). However, Cd^{2+} is less effective in blocking the tail current than it is in blocking the current during the pulse. As shown in Fig. 3, Cd^{2+} (0·1 mM) blocks over 95 % of the Ca current recorded at +20 mV, but it blocks

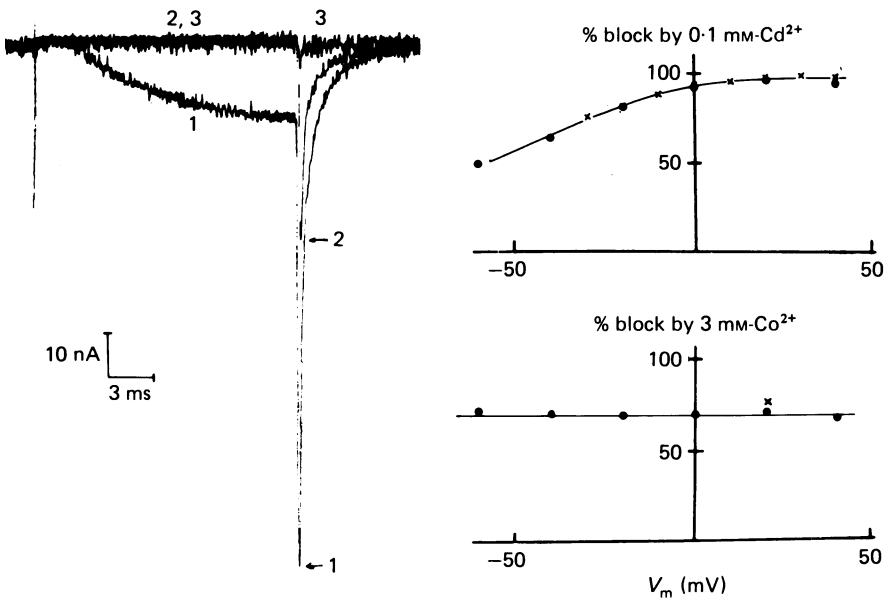

Fig. 3. Block of Ca current by Cd^{2+} and Co^{2+}. Three current records obtained during an 18 ms pulse to +20 mV with a holding potential of −50 mV. Pulse begins at artifact seen about 2 ms from start of records. External solution was normal Tris saline for record 1, Tris saline plus 0·1 mM-Cd^{2+} for record 2, and Co/Tris saline (8 mM-Co^{2+} replaced all Ca^{2+} and Mg^{2+}) for record 3. Arrows indicate peak tail currents. Plots give percentage of Ca current blocked by 0·1 mM-Cd^{2+} or 3 mM-Co^{2+}, current during pulse (×) and peak tail current (●).

only 60 % of the peak tail current (see arrows). The percentage of the peak tail current blocked by 0·1 mM-Cd^{2+} is plotted (●) in Fig. 3 as a function of the membrane potential at which the tail current was recorded. The Cd block of the tail current becomes more complete as the potential becomes more positive. The percentage of the Ca current recorded during the pulse that is blocked by 0·1 mM-Cd^{2+} is also plotted (×) as a function of the membrane potential of the pulse (Fig. 3). The data for the blocking action of Cd^{2+} on the pulse current and on the tail current superimpose, thus supporting the conclusion that the tail current flows through the Ca channels. Such a voltage dependency of the block of Ca current by Cd^{2+} has been suggested by Wilson, Tsuda & Brown (1982). The block of Ca currents by Co^{2+} shows no voltage dependence, as is illustrated by a plot of the percentage of the Ca tail current blocked by 3 mM-Co^{2+} in Fig. 3.

The last argument for the identification of the early tail current as a Ca current is that the smallest positive pulse that causes the activation of a Ca current during

the pulse is also the smallest pulse that elicits the tail current. As is shown in Fig. 4, the Ca current during the pulse (●) and the peak tail current (○) are first clearly detectable for a pulse to −20 mV. (Note that the peak tail current has been divided by 10 in Fig. 4*A*, to make it comparable to the other currents plotted.) Both currents increase in size as the pulse potential is made more positive, up to a potential of

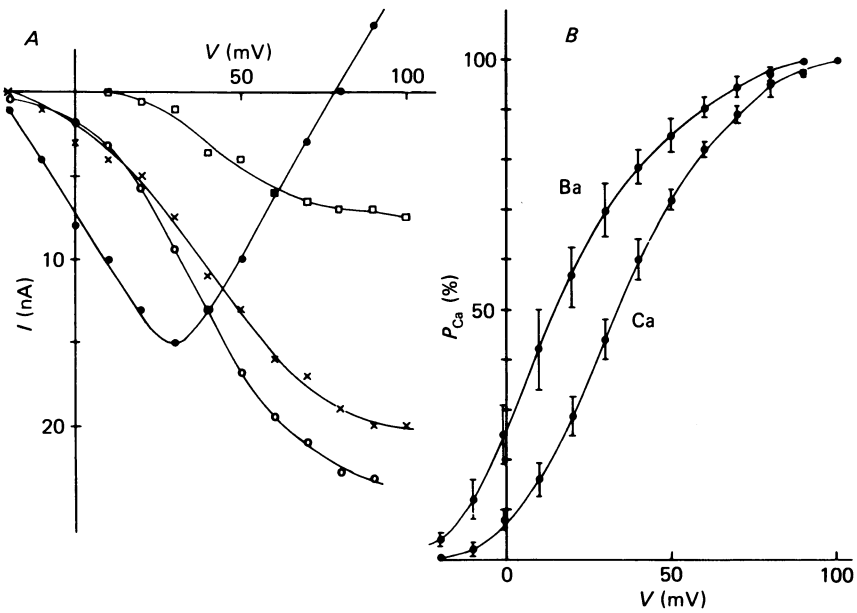

Fig. 4. Voltage dependence of Ca current activation. *A*, data from one cell taken from currents recorded during 15 ms positive voltage pulses to various potentials; holding potential was −50 mV. Ca current during the pulse, at end, (●) and tail current at peak (○), at 1·5 ms (×), and at 6 ms (□). Peak tail current (○) is 10 times larger than indicated by ordinate scale. *B*, percentage of Ca permeability activated plotted against membrane potential. Each point is the mean of the normalized peak tail currents recorded following a pulse to that membrane potential. Error bars indicate standard deviation of the data. Ca data taken from four cells; Ba data taken from three cells.

+30 mV. Above +30 mV, further increase in the pulse potential causes a decrease in the Ca current recorded during the pulse, even though the Ca tail current still increases. This drop in Ca current during the pulse presumably results from the decrease in driving force on Ca^{2+} as the pulse potential becomes more positive. (The tail current, of course, is always measured at the same potential, −50 mV.) The currents recorded during pulses to potentials above +50 mV are badly contaminated by outward currents (carried mainly by H^+) that pass through distinct channels (L. Byerly, R. W. Meech & W. J. Moody, unpublished results); these contaminating currents cause the reversal seen at +80 mV in Fig. 4*A*. The tail current at 6 ms (□) has a dependence on the pulse potential which is different from that of the tail current at the peak (○) and at 1·5 ms (×). This supports our conclusion that the tail current measured at later times after the end of the pulse is contaminated by current flowing through channels other than Ca channels. In the remainder of this paper, it will be assumed that the tail current measured during the first few milliseconds after the end of the positive pulse is flowing through the Ca channel.

Activation of Ca current

Steady-state activation. The current flowing through the membrane at a given potential is directly proportional to the number of open channels. By measuring the size of the tail current obtained when the membrane is stepped from various potentials to −50 mV, we estimate the fraction of the Ca permeability activated at those potentials. We use the peak tail current as the measure of the size of the tail current; this is suitable, since the time course of the Ca tail current is independent of the activating pulse potential. The peak tail current plotted in Fig. 4*A* shows that

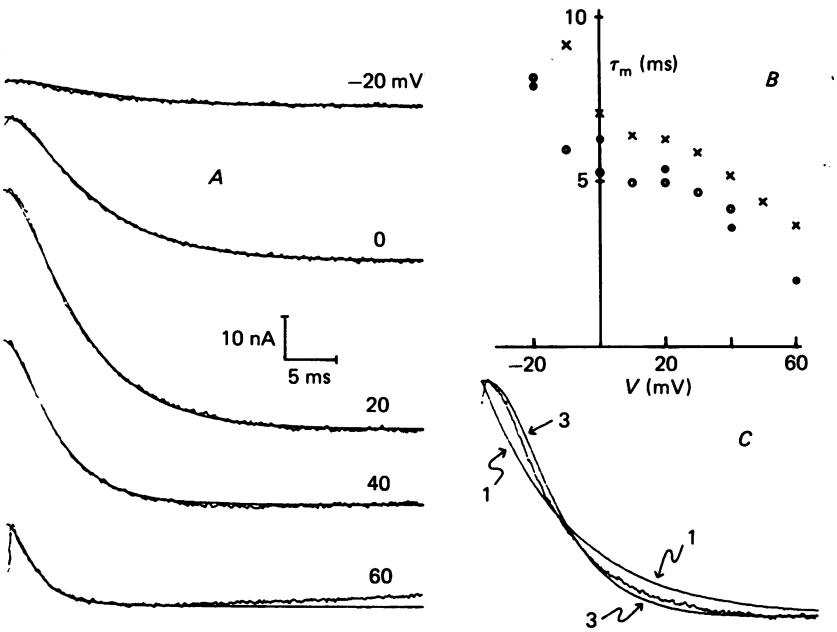

Fig. 5. Time course of Ca current activation. *A*, Ca current records obtained from one cell at the potentials indicated on the records. The positive pulse begins at the left end of the current record. The smooth curve drawn through each record is the m^2 expression fitted to the data. The outward current seen at the beginning of the more positive voltage pulses is thought to be a non-linear, essentially time-independent leakage current; so zero current is taken to be at the peak of this outward current (see Methods). *B*, time constants obtained from the m^2 fit to the data shown in part *A* (●) and to similar data from two other cells (○, ×). *C*, current record for pulse to 20 mV (same as shown in part *A*) with best fits of m^1 form (1) and m^3 form (3). Calibration is the same as for part *A*.

the amount of Ca permeability activated depends on the membrane potential in a sigmoidal manner. The Ca permeability appears to be nearly completely activated at +100 mV. Assuming 100 % activation at +100 mV, we have calculated the means and standard deviations for the data on Ca currents from four cells (plotted in Fig. 4*B*). As can be seen, the Ca permeability is half-activated at 30–35 mV. The maximum Ca current measured during the positive pulse occurs at slightly less positive potentials (20–30 mV).

When Ba^{2+} is substituted for Ca^{2+} as the current carrier, the activation curve is shifted in the negative direction by 15–20 mV (Fig. 4*B*). A similar shift is seen in the

steady-state current–voltage relation (Byerly & Hagiwara, 1982) and probably results from a change in surface potential due to the different binding affinities of Ba^{2+} and Ca^{2+} to the external surface charge. The activating pulses used in collecting all the data for Fig. 4 were 15 ms in duration. As will be seen below, 15 ms allows the Ca (or Ba) current to reach the steady-state value at all except the most negative potentials (−20 mV). In one cell, the activation curve was measured with both 60 and 15 ms pulses; the two curves were essentially identical.

Time course of activation. Fig. 5*A* illustrates the time course with which the Ca current activates when the membrane potential is stepped to levels more positive than the holding potential (−50 mV). The time required for the Ca current to reach the steady-state value clearly decreases as the potential is made more positive. It is also clear that activation does not follow a simple exponential time course of the form $(1-\exp(-t/\tau))$ where τ is the time constant; immediately following the positive step in potential there is a delay before the rapid increase in the Ca current occurs. The non-linear leakage current which turns on in the first few hundred microseconds has no time dependence after 500 μs (see Methods). Traditionally, the activation of the Ca current has been described in terms of the m^x expression used by Hodgkin & Huxley (1952) to fit the Na and K currents of squid axon. In this expression, m is $m_\infty(1-\exp(-t/\tau_m))$ and x is the integer that best fits the time course of activation. We find that the *Lymnaea* Ca current is best fitted by the m^2 form. The smooth curves superimposed on top of the data in Fig. 5*A* are the m^2 fits (see Methods for details). Fig. 5*C* shows the disagreement between the data and the m^1 or m^3 fits for one of the larger Ca currents; the sum of the squared deviations was about 40 times larger for the m^1 fit and 10 times larger for the m^3 fit than for the m^2 fit. For a small number of the current records that we have analysed, the sum of the squares for the m^1 fit or the m^3 fit is as small as that for the m^2 fit, but the m^2 fit is always as good as, if not better than, the m^1 and m^3 fits. The time constant τ_m obtained from the m^2 fit is plotted against potential in Fig. 5*B*. As expected, τ_m decreases as the membrane potential is made more positive.

The Ca current activates with an m^2 time course in response to a step to a particular potential from any holding potential more negative than −50 mV. In the three cells studied, the time course and magnitude of the Ca current obtained on stepping to +20 mV were the same for all holding potentials between −50 and −110 mV. The Ca current obtained from a holding potential of −110 mV was still well fitted by the m^2 form, and the τ_m determined was the same as that found with a holding potential of −50 mV. Thus, over this range of potentials, the Ca current does not demonstrate the phenomenon observed by Cole & Moore (1960) for the squid axon K current. In the squid axon, the delay in the rise of the K current, and the value of x necessary to describe its activation, increase as the holding potential is made more negative. If *Lymnaea* neurones are held at −30 mV, the Ca current obtained on stepping to +20 mV activates with less delay (approaching an m^1 time course) and is smaller than that obtained when neurones are held at −50 mV.

The time course of activation is essentially the same when Ba^{2+} carries the current as when Ca^{2+} carries the current. Ba currents are best fitted by the m^2 form and the values of τ_m determined are similar to those determined for Ca currents at the same potentials (Fig. 6*A*). If there is a 15 mV change in surface potential when Ba^{2+} is

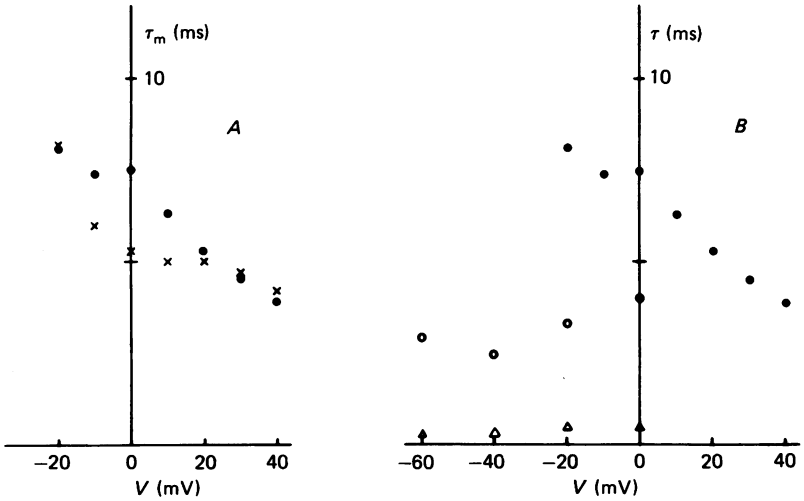

Fig. 6. Time constants for one cell. *A*, time constant of activation τ_m (m^2 fit) for Ca current (×) and Ba current (●) in same cell. *B*, time constants for Ba current activation (●) and fast (△) and slow (○) components of the Ba tail current measured in one cell (same as that of part *A*).

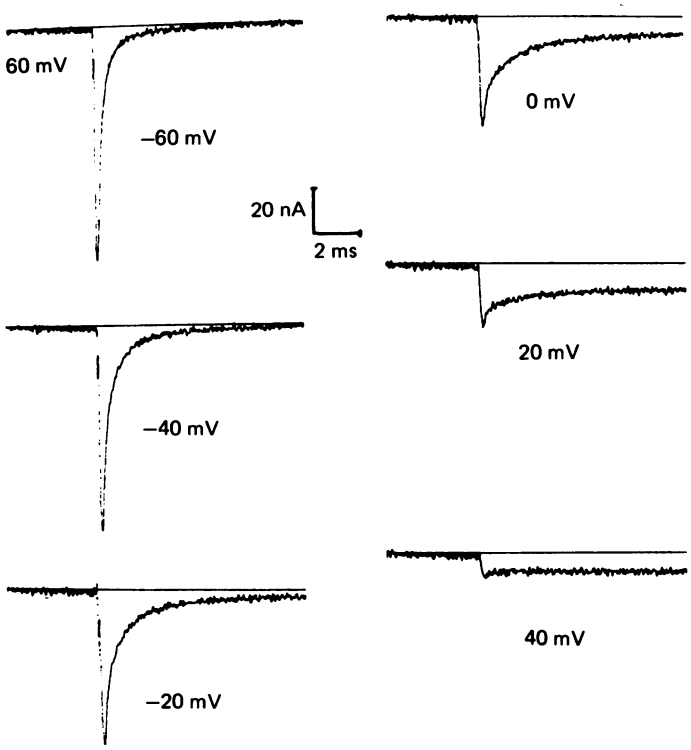

Fig. 7. Ca tail currents measured at various potential levels. Membrane potential was stepped to 60 mV for 8 ms before stepping to the six potentials indicated in the Figure. Current low-pass filter set at 10 kHz. The straight line in each current record indicates the holding current level. Holding potential was −50 mV.

substituted for Ca^{2+} (as suggested by the activation curves in Fig. 4*B*), the time constants determined for Ba currents should be compared to the Ca current time constants measured at potentials that are 15–20 mV more positive. This would make the Ba current seem to activate slightly more slowly than the corresponding Ca current in this particular cell. This sort of comparison of activation of Ba and Ca currents in the same cell has not been done for enough cells to determine if this small difference is significant.

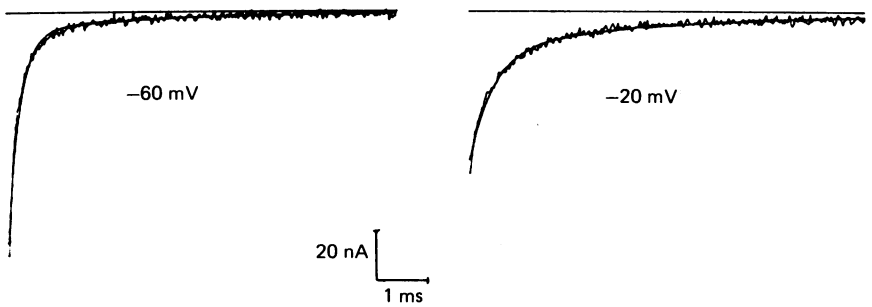

Fig. 8. Curves fitted to Ca tail current. The tail current data (recorded at the potentials indicated in Figure) are from the same experiment as that shown in Fig. 7. The smooth curves superimposed on the data are those fitted by the computer; each consists of two exponential terms and a constant. The data and fitted curves start at 230 μs after the step down from +60 mV. The straight lines indicate the level of the holding current.

Turn-off of Ca current

The time course of the Ca tail current is strongly dependent upon the membrane potential at which the tail current is measured. Fig. 7 gives an example of the currents recorded on stepping the membrane potential down from +60 mV to various levels. The tail current decays much more rapidly at negative potentials than at more positive potentials. The time course of the tail current is more complicated than a single exponential. We have fitted the first 8 ms of current record following the step down from +60 mV with the sum of two decaying exponentials and a constant. As can be seen in Fig. 8, the two-exponential expression gives a reasonably good fit to the tail current data.

The parameters obtained from these fits are plotted against membrane potential in Fig. 9. The plotted data (● with error bars) are the means and standard deviations of the parameters obtained from seven cells. The two time constants are an order of magnitude different in size. The time constant of the fast component, τ_f, shows some voltage dependence, increasing from a little over 200 μs at −60 mV to 400 μs at 0 mv. The time constant associated with the slow component, τ_s, shows no significant voltage dependence and is about 3 ms. The amplitude of each of the two components is given as the magnitude of that term when projected back to the time at which the step occurred. All the amplitudes obtained for one cell have been divided by the amplitude of the fast component at −60 mV in that cell, to normalize the data. The amplitude of the fast component, I_f, decreases rapidly as the membrane potential becomes more positive, while the amplitude of the slow component, I_s, is maximum at −20 mV. Thus, the slower decay of the Ca tail current at more positive potentials results from the larger ratio of the magnitudes of slow to fast component.

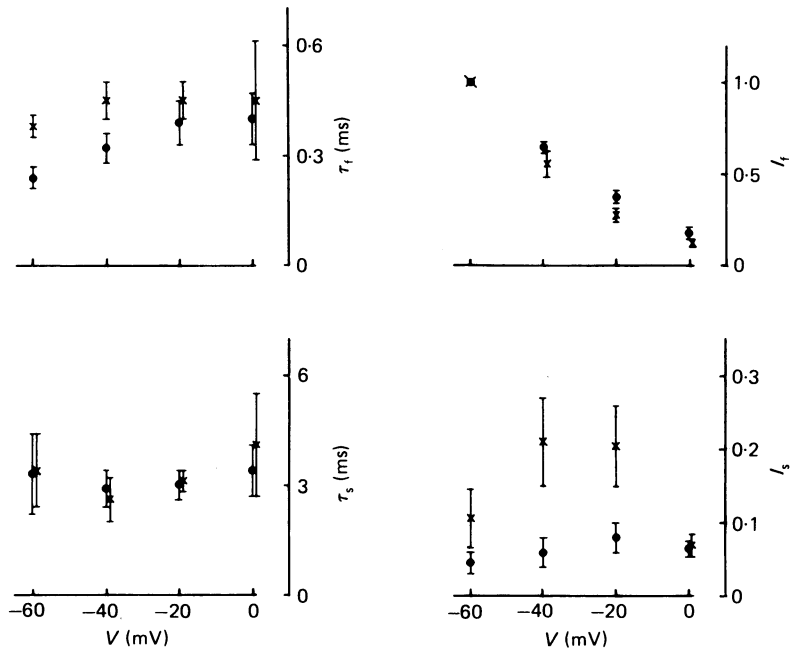

Fig. 9. Parameters of two-exponential fits to tail currents. The point and error bars give the mean and the standard deviation of that parameter for seven cells with external Ca^{2+} (●) or for five cells with external Ba^{2+} (×). τ_f and τ_s are the time constants of the fast and slow components of the tail current. I_f and I_s are the amplitudes of the fast and slow components, projected to the time of the step down in potential. All the current amplitudes for one cell are divided by the value of I_f at −60 mV for that cell, to allow comparison between cells.

We assume that the two exponential terms fitted to the tail current describe the Ca tail current, while the constant term represents slower tail currents (some of which pass through channels other than Ca channels) and steady-state Ca current. Since Ca current has been found to dominate the first 1·5 ms of the tail current (at −50 mV), the fast exponential (τ_f = 0·3 ms) clearly describes the Ca tail current. At 1·5 ms (when the Ca current still dominates), the slow exponential term is much larger than the fast exponential; so the slow exponential must also describe the Ca tail current in at least a rough way. The relatively small standard deviations of the I_s values, which have been normalized to the fast component, support the conclusion that the slow component is closely related to the fast component and is not an independent current. (The ratio of the amplitudes of two independent currents in these cells can vary greatly from cell to cell; see Stimers & Byerly, 1982.)

The time course of Ba tail currents, obtained when external Ca^{2+} has been replaced by Ba^{2+}, is very similar to that of the Ca tail currents. The parameters obtained by fitting the Ba tail currents from five cells are also shown in Fig. 9 (×). τ_s is the same for Ba tail currents as for Ca currents. τ_f is significantly larger for Ba currents than for Ca currents at −60 and −40 mV; however, the shift of the Ba current activation kinetics by 15–20 mV in the negative direction could explain this difference. The dependence of I_f on voltage is about the same for Ba as for Ca, but the slow component

(I_s) of the Ba tail current is significantly larger than that of the Ca tail current. The explanation for this difference might lie in the greater effectiveness of intracellular Ca^{2+} over intracellular Ba^{2+} in blocking Ca channels (Tillotson, 1979). The influx of Ca^{2+} during the large fast component of the tail current could block a significant fraction of the Ca channels, so the slow component of the Ca tail current would be reduced. There would be less of such an effect with Ba tail currents. The extent to which accumulation of intracellular Ca^{2+} plays a role in determining the time course of the tail currents will be discussed further in the Discussion section.

Model for activation

The data we have obtained on the activation and the turn-off of Ca current are consistent with a linear sequential model with at least three closed states and one open state:

$$C_1 \rightleftharpoons C_2 \rightleftharpoons C_3 \rightleftharpoons O.$$

This model is described by a system of differential equations, the solution of which involves the sum of three exponentials (+ or − amplitudes). Since our data demonstrate the existence of at least three different time constants at one voltage, no simpler model can account for the data. At 0 mV, the tail current has exponential components with time constants of 0·4 and 3 ms (Fig. 9). The activation at 0 mV is described by m^2 kinetics with a time constant of 6 ms (Fig. 5); this implies two components with time constants of 6 and 3 ms. Values for τ_m, τ_f, and τ_s that are all measured in the same cell are plotted in Fig. 6*B*. It is clear that at least three distinct time constants are necessary to describe the Ca current activation kinetics.

The slow nature of activation and the fast component of the tail current can be explained by assuming that the transitions between closed states occur more slowly than the transitions between the closed state C_3 and the open state. When the membrane potential is held at −50 mV or a more negative value, most of the Ca channels are in state C_1; a step to positive potentials gives a slow m^2 activation because the channels have to make the two slow transitions before they can reach the open state. Once in the open state, the channels only have to make the fast transition to state C_3 to stop carrying current, giving the fast tail current. When the membrane potential is held at −30 mV, the Ca current activates with roughly m^1 kinetics. This suggests that, at −30 mV, a large fraction of the Ca channels are in state C_2 and only have to make one slow transition to reach the open state.

This qualitative model for the Ca current activation suggests an experiment. If the membrane is stepped positive after the fast component of the tail has decayed but while the slow component is still present, the resulting turn-on of the Ca current should occur more rapidly than usual, because many of the Ca channels would be in states C_3 and C_2 when the positive step occurs. Fig. 10 shows the results obtained when we stepped the membrane to +20 mV a short time after a pulse to +60 mV, separating the two pulses by a return to −50 mV for 1–10 ms. When the interval is 1 ms, the Ca current activated by the second pulse rises very abruptly; half of the current that is turned on by the second pulse is activated in less than 3 ms. When the interval is 10 ms, the Ca current activates with the usual m^2 kinetics, requiring over 6 ms to reach half of the maximum current. Oxford (1981) found that the Na current also activates abruptly, without its characteristic delay, when a second activating pulse closely follows the end of a first.

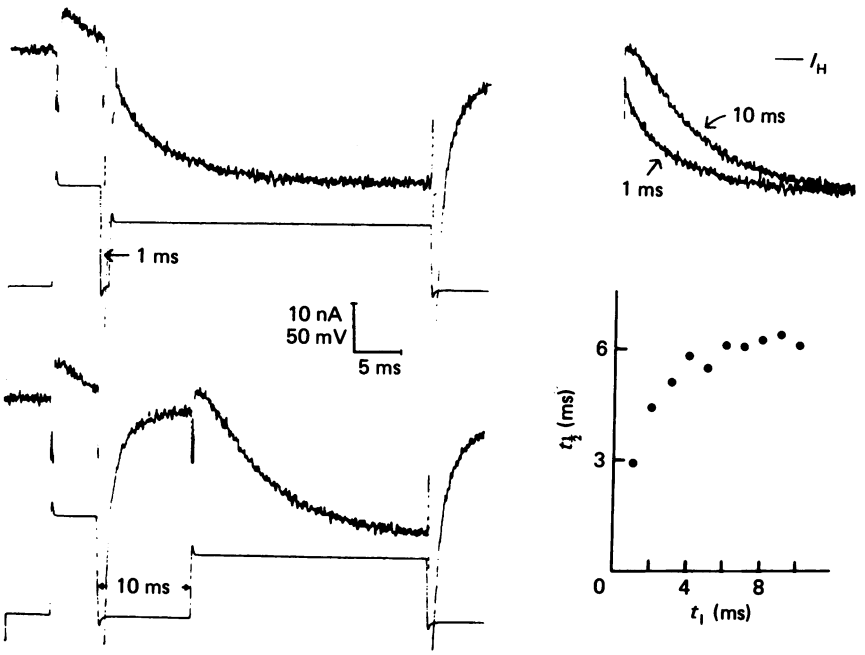

Fig. 10. Reactivation of Ca current. In this experiment, the membrane potential, which is plotted below the current for the two current records shown at the left, is stepped from the holding potential of −50 mV to 60 mV for 5 ms, then back to −50 mV for a variable length of time t_I, and then to 20 mV. Upper left, t_I = 1 ms. Lower left, t_I = 10 ms. Upper right, the activations of the Ca current at 20 mV in the two current records at left are shown in juxtaposition; the records have been shifted in time so that the steps from −50 to 20 mV are superimposed. Line marked I_H indicates level of holding current. Lower right, plot of $t_{\frac{1}{2}}$, the time required for the Ca current to make half of the change from its value at the beginning of the pulse to the steady-state value, against t_I.

Open-channel I–V relation

Experiments of the type shown in Fig. 7, in which the membrane potential is stepped to various potentials following a pulse to +60 mV, allow us to determine the *I–V* relation for open Ca channels. If the potential change occurred instantaneously and if the current could be measured immediately after the step, that current plotted against the potential at which it was measured would directly give the open-channel *I–V* relation, because the current would be measured before the gating mechanism of the channel could respond to the voltage change. However, in our experiments, the voltage change requires 150–300 μs to be completed. We estimate an instantaneous current by projecting the two-exponential fit back to the time at which the step began; most of the potential change occurs in the first 50 μs. The filled dots in the plots in Fig. 11 show the open-channel *I–V* relation obtained in this manner. This relation can be determined in a second way for those potentials at which a significant number of Ca channels are open in the steady state. This method involves measuring the Ca current at the end of the positive pulse and then the size of the Ca tail current on returning to the holding potential, for positive pulses to a range of potentials. Fig. 4*A* shows the results of such an experiment. The ratio of the Ca current at the end of the pulse to the peak tail current plotted against the pulse potential gives the open-channel *I–V* relation for positive membrane potentials. The *I–V* relations

determined in this second manner are also plotted (×) in Fig. 11. In this Figure, the currents determined in the first manner (●) have been normalized so as to give the best agreement with the data obtained by the second method (×). No data are plotted for potentials above +50 mV, since the Ca currents are seriously contaminated by currents flowing through channels other than the Ca channel at potentials above 40–50 mV.

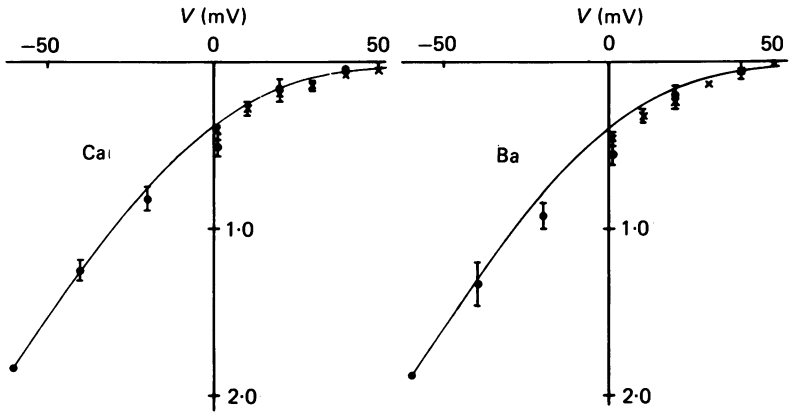

Fig. 11. Open-channel I–V relations for the Ca channel. Current is carried by Ca^{2+} (at left) and by Ba^{2+} (at right). The data points come from two sources, the ratio of pulse current to tail current (×) from experiments like that of Fig. 4*A*, and the instantaneous current (●) on stepping down from +60 mV as in Fig. 7. The instantaneous current data have been scaled to give the best fit to the ratio data in the region of overlap. The points and error bars indicate the mean and standard deviation of the data from seven cells for Ca instantaneous points, five cells for Ba instantaneous points, three cells for Ca ratio points and three cells for Ba ratio points. Since the instantaneous data for each cell were normalized by the value at −60 mV, no error bars are shown for the −60 mV points. The smooth curves are the relations predicted by the constant-field expression

$$I \propto V\exp(-2FV/RT)/(1-\exp(-2FV/RT)),$$

where the proportionality constant is chosen so that the curve goes through the point at −60 mV, and F, R and T have their usual meanings.

The open-channel I–V relations determined for Ca and Ba currents are very similar (Fig. 11). Both relations show a negative curvature in the sense expected from the much higher concentration of Ca^{2+} (or Ba^{2+}) outside the membrane than inside. The smooth curves drawn in Fig. 11 show the I–V relation predicted by the constant-field relation. Considering that the Ca channel is known not to satisfy the independence relation (Hagiwara & Byerly, 1981) and that the potential we measure is not the true transmembrane potential (due to surface potentials), there is little reason to expect our open-channel I–V relation to fit the constant-field expression. We use the constant-field expression because it contains only a single adjustable parameter, which we have chosen so that the curve passes through the data at −60 mV. The agreement of the data with the constant-field relation is surprisingly good.

DISCUSSION

Temperature dependence

We found the Ca current in *Lymnaea* neurones to be quite sensitive to temperature. Our value for the Q_{10} of the reciprocal of the time constant of activation, 4·9, is considerably larger than the value of 2·6 obtained by Kostyuk, Krishtal & Pidoplichko (1981) for the Ca current of *Helix* neurones or the values of 2·0–2·6 measured by Kimura & Meves (1979) for the squid axon Na current. However, Kimura & Meves found that the Q_{10} of the reciprocal of τ_h, the inactivation time constant, reached values of 3·3–4·9 between 0 and 10 °C, which is comparable to the Q_{10} of τ_m reported here. We found that the time course of the Ca tail current is also slowed by lowering the temperature; this result is at odds with the report of Wilson *et al.* (1982) that the rate of decay of the Ca tail currents in *Helix* neurones is unchanged between 14 and 23 °C.

When temperature is lowered, the amplitude of the maximum Ca current in *Lymnaea* falls with a Q_{10} of 2·3. This is similar to the value of 2·0 determined for *Helix* Ca current (Kostyuk *et al.* 1981). Kimura & Meves (1979) found that the Q_{10} of the peak Na current in squid axon depended on temperature, being 1·6–2·0 for 10–15 °C and 1·9–3·9 for 0–10 °C. The Q_{10} we measured for the maximum Ca current may not indicate the temperature sensitivity of the permeability of an open Ca channel, because the number of conducting Ca channels in the membrane may drop with temperature, even though there is no apparent shift of activation with temperature. Plant, Standen & Ward (1983) have shown that the normal level of Ca^{2+} inside snail neurones is high enough to block a fraction of the Ca channels. Lowering the temperature might slow the mechanisms that extrude or sequester Ca^{2+} sufficiently to cause an increase in the level of intracellular Ca^{2+}, which would reduce the number of conducting Ca channels. Recordings from Ca-sensitive micro-electrodes have shown that the concentration of Ca^{2+} just inside the membrane of our cells is considerably higher than that of the internal perfusion solution, which contains 5 mM-EGTA (Byerly & Moody, 1983). In addition, the number of conducting Ca channels might be expected to change with temperature if there are intracellular chemical reactions that interconvert the Ca channel between functionally different states, as seems to be the case for cardiac Ca channels (Reuter, 1983).

Cadmium block

The voltage dependence of the block of Ca current by Cd^{2+} is unusual in its direction. In most cases of voltage-dependent blocking, the blocker becomes more effective at potentials that tend to drive the blocker into the channel. External Cd^{2+} blocks less effectively at more negative potentials, at which it is more strongly driven into the Ca channel. Since Cd^{2+} has been reported to pass through the Ca channels in larval insect muscle (Fukuda & Kawa, 1977) and frog skeletal muscle (Palade & Almers, 1978), we are led to speculate that the Cd block is reduced at negative potentials because Cd^{2+} is driven through the channel by the large driving force. Co^{2+}, an ion which has not been observed to pass through the Ca channel, blocks the Ca current in a voltage-independent manner.

Voltage dependence of activation

The voltage dependence of the fraction of Ca permeability activated, as determined by the size of the tail current (Fig. 4*B*), has also been determined in pituitary cells (Hagiwara & Ohmori, 1982) and chromaffin cells (Fenwick *et al.* 1982). In all three cases, the Ca permeability is only about half activated at the potential at which the maximum steady-state current is recorded; in the two secretory cells, the maximum current is recorded at potentials at which a little over half of the Ca permeability is activated, while in *Lymnaea*, a little less than half of the Ca permeability is activated when the maximum Ca current is recorded. The voltage dependence of activation is steeper in the secretory cells, going from 10 to 90 % activation with a 50 mV increase in potential. The same range of activation spans 70 mV in *Lymnaea*.

Open-channel I–V relation

The open-channel *I–V* relation that we determined (Fig. 11) agrees fairly well with that found for the chromaffin cell (Fenwick *et al.* 1982). We do not extend our curve above +50 mV, because we think the currents during the pulse are seriously contaminated by currents not going through the Ca channel at very positive potentials. These contaminating currents appear to be mostly carried by H^+ through distinct channels (L. Byerly, R. W. Meech & W. J. Moody, unpublished results). The open-channel *I–V* curves for chromaffin cells and *Lymnaea* neurones both exhibit negative curvature at positive potentials and approach a straight line of large positive slope at negative potentials, as is predicted by the constant-field equation. The *I–V* relation shows no indication of saturation at negative potentials as has been reported in some studies (Llinas, Steinberg & Walton, 1981). Such an apparent saturation would be expected if the fast tail current were not detected.

Time course of activation

The results of this study of Ca current activation at low temperatures are completely consistent with the results obtained with the same preparation at room temperature (Byerly & Hagiwara, 1982); however, the fact that activation is slowed by a factor of 7–10 allows us to establish that the time course follows m^2 kinetics with much greater confidence (Fig. 5*A* and *C*). The activation of Ca currents in *Helix* neurones (Kostyuk *et al.* 1981) and in pituitary cells (Hagiwara & Ohmori, 1982) has also been shown to follow m^2 kinetics. At 10 °C, the time constant of activation (τ_m) at 0 mV is 5–8 ms in *Helix* neurones, pituitary cells, and *Lymnaea* neurones. In all three types of cells, τ_m decreases monotonically with membrane potential.

It is difficult to compare the time course of chromaffin cell Ca currents with our results, because Fenwick and co-workers (1982) have fitted the data with a three-exponential form, instead of the m^x expression. Since our activation data are well fitted by an expression that has a single free parameter, we have no motivation for fitting with an expression that has three or more degrees of freedom. Of course, Fenwick and co-workers have considerable additional information from fluctuation analysis and single-channel recordings that we do not. One puzzling feature of the activation time constants obtained for the chromaffin cell data is that the time constant of the major component reaches a maximum near the potential at which

the current amplitude is maximum. The τ_m fitted to the data from pituitary cells or snail neurones shows no such maximum.

Time course of Ca tail currents

Most studies of Ca currents have not seen the fast component of the Ca tail current. When the Ca tail current appears as a single exponential with a time constant that is not very different from the time constant of activation, the voltage clamp is probably not fast enough to resolve the fast component. Hagiwara & Ohmori (1982) suggest that this is the case in their study of pituitary cells. The fast component of the Ca tail current has been reported in *Helix* neurones (Tsuda *et al.* 1982), chromaffin cells (Fenwick *et al.* 1982), and rod photoreceptors (Corey, Dubinsky & Schwartz, 1982), as well as *Lymnaea* neurones. At negative potentials near the holding level, the fast component is much larger than the slow component. The ratio of the amplitudes (fast:slow) at the holding potential (-50 to -70 mV) is 4:1 or greater in snail neurones and chromaffin cells. This ratio has been shown to decrease rapidly as the membrane potential becomes more positive. The two components have time constants in the ratio of about 10:1 for both *Helix* and *Lymnaea* neurones, while their ratio is about 4:1 in chromaffin cells. The fast time constant increases with membrane potential in both *Lymnaea* neurones and chromaffin cells. The slow time constant remains unchanged between -60 and 0 mV in *Lymnaea*; however, it increases by a factor of 5 between -70 and -10 mV in chromaffin cells.

It is interesting to compare the fast tail time constant to the mean open time found from single-channel Ca recordings. The Ca channel mean open time is about 1 ms in all cells studied: cardiac cells at 25 °C (Reuter *et al.* 1982), chromaffin cells at 20–22 °C (Fenwick *et al.* 1982), and pituitary cells at 8–10 °C (Hagiwara & Ohmori, 1983); the mean open time was estimated to be 2·5 ms in *Helix* neurones (Lux & Nagy, 1981). The mean open time for a single channel should be larger than the fast tail time constant, since for a two-state model the time constant of the tail current is the reciprocal of the sum of the two rate constants while the mean open time is the reciprocal of only the off rate constant. The presence of additional closed states in the four-state model which is outlined in the Results section would decrease the fast tail time constant without affecting the mean open time. Since the fast tail time constant is less than 0·5 ms in both chromaffin and *Lymnaea* cells, the data fit the expected relation between the fast tail time constant and the mean open time.

The fact that the time constants for Ba tail currents are about the same as those for Ca tail currents argues that accumulation of Ca^{2+} inside the membrane does not strongly affect the measured time course of the tail currents. Intracellular Ba^{2+} appears to be considerably less effective than Ca^{2+} in blocking the Ca channel (Eckert & Tillotson, 1981). After allowing for the 15–20 mV surface potential shift that appears when Ba^{2+} replaces Ca^{2+}, there is less than a 20 % increase in τ_f and no change in τ_s (Fig. 9). Another argument against the idea that Ca accumulation might contribute to make τ_f small lies in the observation that τ_f is relatively independent of the magnitude of the Ca tail current. Modelling shows that as Ca currents get larger, their rate of decay due to Ca accumulation should get faster (Plant *et al.* 1983). The size of the Ca tail currents recorded at the holding potential can be varied by changing the amplitude (Fig. 4*A*) or the duration (Fig. 2) of the positive pulse. We have

determined τ_f for the Ca tail currents from both types of experiments and find that τ_f is essentially the same for all records, although the amplitude of the tail current changes by a factor of 10.

Kinetic model for Ca channel activation

There is little agreement at this time as to what is the appropriate model for Ca channel activation. The data we present here are consistent with a four-state, linear sequential model with three closed states and a single open state:

$$C_1 \rightleftharpoons C_2 \rightleftharpoons C_3 \rightleftharpoons O. \quad (1)$$

Our data suggest that the transitions between the closed states can be represented by a Hodgkin–Huxley type formalism (specifically m^2), while the transition between the open state and the last closed state (C_3) has a time constant which is an order of magnitude smaller than the time constants of the other transitions. A similar model has been suggested by Wilson, Brown & Tsuda (1983). Hagiwara & Ohmori (1983) favour a slightly different scheme for the four-state model:

$$C_1 \rightleftharpoons C_2 \rightleftharpoons O \rightleftharpoons C_3. \quad (2)$$

As Hagiwara & Ohmori point out, this model cannot account for the time course of the Ca tail current, but it does have certain advantages for fitting their single-channel data.

Fenwick and co-workers (1982) proposed a simple three-state model:

$$C_1 \rightleftharpoons C_2 \rightleftharpoons O. \quad (3)$$

Since they needed three time constants to fit the activation of the Ca current, this three-state model cannot be a complete one, but they were able to fit it to a large amount of the data from macroscopic, single-channel, and noise analyses. In an effort to describe our data by such a three-state model we tried to fit the activation time course with a two-exponential form in which the time constants were constrained to differ by a factor of 10, the ratio between the two tail current time constants (τ_f and τ_s). Such a two-exponential form fits the data badly; it is only slightly better than the m^1 fit. The three-state model is not consistent with our data.

We gratefully acknowledge the assistance of Drs Susumu Hagiwara and Sally Krasne in the preparation of this manuscript. This work was supported by a U.S.P.H.S. grant (NS 15341) to Dr Byerly and an American Heart Association Research Fellowship to Dr Stimers.

REFERENCES

BYERLY, L. & HAGIWARA, S. (1981). Isolation of calcium current in internally dialyzed snail neurons. *Biophys. J.* **33**, 143a.

BYERLY, L. & HAGIWARA, S. (1982). Calcium currents in internally perfused nerve cell bodies of *Limnaea stagnalis*. *J. Physiol.* **322**, 503–528.

BYERLY, L. & MOODY, W. J. (1983). Intracellular Ca^{++} and Ca currents in internally perfused snail neurons. *Biophys. J.* **41**, 292a.

COLE, K. S. & MOORE, J. W. (1960). Potassium ion current in the squid giant axon: dynamic characteristic. *Biophys. J.* **1**, 1–14.

COREY, D. P., DUBINSKY, J. & SCHWARTZ, E. A. (1982). The calcium current of rod-photoreceptor inner segments recorded with a whole-cell patch clamp. *Neurosci. Abstr.* **8**, 944.

ECKERT, R. & TILLOTSON, D. L. (1981). Calcium-mediated inactivation of the calcium conductance in caesium-loaded giant neurones of *Aplysia californica*. *J. Physiol.* **314**, 265–280.

FENWICK, E. M., MARTY, A. & NEHER, E. (1982). Sodium and calcium channels in bovine chromaffin cells. *J. Physiol.* **331**, 599–635.

FUKUDA, J. & KAWA, K. (1977). Permeation of manganese, cadmium, zinc, beryllium through calcium channels of an insect muscle membrane. *Science, N.Y.* **196**, 309–311.

HAGIWARA, S. & BYERLY, L. (1981). Calcium channel. *Ann. Rev. Neurosci.* **4**, 69–125.

HAGIWARA, S. & OHMORI, H. (1982). Studies of calcium channels in rat clonal pituitary cells with patch electrode voltage clamp. *J. Physiol.* **331**, 231–252.

HAGIWARA, S. & OHMORI, H. (1983). Studies of single calcium channel currents in rat clonal pituitary cells. *J. Physiol.* **336**, 649–661.

HAMILL, O. P., MARTY, A., NEHER, E., SAKMANN, B. & SIGWORTH, F. J. (1981). Improved patch-clamp techniques for high-resolution current recording from cells and cell-free membrane patches. *Pflügers Arch.* **391**, 85–100.

HODGKIN, A. L. & HUXLEY, A. F. (1952). A quantitative description of membrane current and its application to conduction and excitation in nerve. *J. Physiol.* **117**, 500–544.

KIMURA, J. E. & MEVES, H. (1979). The effect of temperature on the asymmetrical charge movement in squid giant axons. *J. Physiol.* **289**, 479–500.

KOSTYUK, P. G., KRISHTAL, O. A. & PIDOPLICHKO, V. I. (1981). Calcium inward current and related charge movements in the membrane of snail neurones. *J. Physiol.* **310**, 403–421.

KOSTYUK, P. G., KRISHTAL, O. A. & SHAKHOVALOV, Y. A. (1977). Separation of sodium and calcium currents in the somatic membrane of mollusc neurones. *J. Physiol.* **270**, 545–568.

KRISHTAL, O. A. & PIDOPLICHKO, V. I. (1975). Intracellular perfusion of *Helix* giant neurons. *Neirofiziologiya* **7**, 327–329, translated in *Neurophysiology* **7**, 258–259 (1976).

LEE, K. S., AKAIKE, N. & BROWN, A. M. (1978). Properties of internally perfused, voltage-clamped, isolated nerve cell bodies. *J. gen. Physiol.* **71**, 489–507.

LLINAS, R., STEINBERG, I. Z. & WALTON, K. (1981). Presynaptic calcium currents in squid giant synapse. *Biophys. J.* **33**, 289–322.

LUX, H. D. & NAGY, K. (1981). Single channel Ca^{2+} currents in *Helix pomatia* neurons. *Pflügers Arch.* **391**, 252–254.

OXFORD, G. S. (1981). Some kinetic and steady-state properties of sodium channels after removal of inactivation. *J. gen. Physiol.* **77**, 1–22.

PALADE, P. T. & ALMERS, W. (1978). Slow Na and Ca currents across the membrane of frog skeletal muscle fibers. *Biophys. J.* **21**, 168a.

PLANT, T. D., STANDEN, N. B. & WARD, T. A. (1983). The effects of injection of calcium ions and calcium chelators on calcium channel inactivation in *Helix* neurones. *J. Physiol.* **334**, 189–212.

REUTER, H., STEVENS, C. F., TSIEN, R. W. & YELLEN, G. (1982). Properties of single calcium channels in cardiac cell culture. *Nature, Lond.* **297**, 501–504.

REUTER, H. (1983). Calcium channel modulation by neurotransmitters, enzymes, and drugs. *Nature, Lond.* **301**, 569–574.

STIMERS, J. R. & BYERLY, L. (1982). Slowing of sodium current inactivation by ruthenium red in snail neurons. *J. gen. Physiol.* **80**, 485–497.

TAKAHASHI, K. & YOSHII, M. (1978). Effects of internal free calcium upon the sodium and calcium channels in the tunicate egg analysed by the internal perfusion technique. *J. Physiol.* **279**, 519–549.

TILLOTSON, D. (1979). Inactivation of Ca conductance dependent on entry of Ca ions in molluscan neurons. *Proc. natn. Acad. Sci. U.S.A.* **76**, 1497–1500.

TSUDA, Y., WILSON, D. L. & BROWN, A. M. (1982). Calcium tail currents in snail neurons. *Biophys. J.* **37**, 181a.

WILSON, D. A., BROWN, A. M. & TSUDA, Y. (1983). Modeling of Ca current activation. *Biophys. J.* **41**, 61a.

WILSON, D. L., TSUDA, Y. & BROWN, A. M. (1982). Activation of Ca channels in snail neurons. *Biophys. J.* **37**, 181a.